AD_____

Award Number: DAMD17-98-1-8570

TITLE: Identification of Novel Oncogenes in Carcinoma of the
       Prostate

PRINCIPAL INVESTIGATOR: John M. Ruppert, M.D.

CONTRACTING ORGANIZATION: University of Alabama at Birmingham
                          Birmingham, Alabama   35294-3300

REPORT DATE: September 1999

TYPE OF REPORT: Annual

PREPARED FOR: U.S. Army Medical Research and Materiel Command
               Fort Detrick, Maryland   21702-5012

DISTRIBUTION STATEMENT: Approved for public release;
                        Distribution Unlimited

The views, opinions and/or findings contained in this report are
those of the author(s) and should not be construed as an official
Department of the Army position, policy or decision unless so
designated by other documentation.

20000809 079

REPORT DOCUMENTATION PAGE

OMB No. 074-0188

1. AGENCY USE ONLY (Leave blank)	2. REPORT DATE September 1999	3. REPORT TYPE AND DATES COVERED Annual (1 Sep 98 – 31 Aug 99)

4. TITLE AND SUBTITLE Identification of Novel Oncogenes in Carcinoma of the Prostate	5. FUNDING NUMBERS DAMD17-98-1-8570

6. AUTHOR(S)
John M. Ruppert, M.D.

7. PERFORMING ORGANIZATION NAME(S) AND ADDRESS(ES) University of Alabama at Birmingham Birmingham, Alabama 35294-3300 E-MAIL: mruppert@uab.edu	8. PERFORMING ORGANIZATION REPORT NUMBER

9. SPONSORING / MONITORING AGENCY NAME(S) AND ADDRESS(ES) U.S. Army Medical Research and Materiel Command Fort Detrick, Maryland 21702-5012	10. SPONSORING / MONITORING AGENCY REPORT NUMBER

11. SUPPLEMENTARY NOTES

Report contains color graphics.

12a. DISTRIBUTION / AVAILABILITY STATEMENT Approved for public release; distribution unlimited	12b. DISTRIBUTION CODE

13. ABSTRACT (Maximum 200 Words)

A cell line termed RK3E provides a novel approach to identification and functional analysis of carcinoma-derived transforming oncogenes. Derived by immortalization of primary rat kidney cells, RK3E exhibit multiple properties of epithelia and specifically detect the tranforming activity a small subset of all oncogenes, including c-MYC, RAS, β-catenin, and the zinc finger proteins GLI and GKLF. Strikingly, the conventional host for oncogene isolation, NIH3T3 cells, detects the activity of just one of these carcinoma-relevant oncogenes, the G protein RAS. GKLF was recently identified as a novel RK3E transforming oncogene and was found to be expressed at elevated levels in dysplastic epithelium in vivo. These results suggest that carcinoma types for which oncogenes are poorly characterized can be rapidly assessed for novel transforming oncogenes, and that such genes are likely to be relevant to tumor progression in vivo. For analysis of oncogenes expressed in prostate cancer, we have purified polyA+ mRNA and begun preparation of cDNA libraries.

14. SUBJECT TERMS Prostate Cancer			15. NUMBER OF PAGES 20
			16. PRICE CODE

17. SECURITY CLASSIFICATION OF REPORT Unclassified	18. SECURITY CLASSIFICATION OF THIS PAGE Unclassified	19. SECURITY CLASSIFICATION OF ABSTRACT Unclassified	20. LIMITATION OF ABSTRACT Unlimited

NSN 7540-01-280-5500

Standard Form 298 (Rev. 2-89)
Prescribed by ANSI Std. Z39-18
298-102

FOREWORD

Opinions, interpretations, conclusions and recommendations are those of the author and are not necessarily endorsed by the U.S. Army.

JMR Where copyrighted material is quoted, permission has been obtained to use such material.

___ Where material from documents designated for limited distribution is quoted, permission has been obtained to use the material.

___ Citations of commercial organizations and trade names in this report do not constitute an official Department of Army endorsement or approval of the products or services of these organizations.

X In conducting research using animals, the investigator(s) adhered to the "Guide for the Care and Use of Laboratory Animals," prepared by the Committee on Care and use of Laboratory Animals of the Institute of Laboratory Resources, national Research Council (NIH Publication No. 86-23, Revised 1985).

X For the protection of human subjects, the investigator(s) adhered to policies of applicable Federal Law 45 CFR 46.

N/A In conducting research utilizing recombinant DNA technology, the investigator(s) adhered to current guidelines promulgated by the National Institutes of Health.

N/A In the conduct of research utilizing recombinant DNA, the investigator(s) adhered to the NIH Guidelines for Research Involving Recombinant DNA Molecules.

N/A In the conduct of research involving hazardous organisms, the investigator(s) adhered to the CDC-NIH Guide for Biosafety in Microbiological and Biomedical Laboratories.

_____   9/22/99
PI Signature   Date

3

TABLE OF CONTENTS:

Introduction:

Transforming oncogenes have traditionally been identified by introduction of tumor DNA or cDNA into mesenchymal cells such as NIH3T3. We have developed an expression cloning assay using an epithelial cell line that serves to identify oncogenes expressed in carcinomas in a sensitive and specific fashion. These cells form foci when transduced with activated RAS, activated β-catenin, or wild type alleles of c-MYC, GLI, or GKLF. In contrast, NIH3T3 cells form foci in response to RAS, but exhibit no response to any the other major carcinoma oncogenes listed above. As few oncogenes are known to be activated in prostate cancer, we will apply the RK3E assay to human prostate tumor cell lines. By analogy with a recently completed and published screen of breast and oral cancer lines, we expect to identify c-MYC as well as other known or novel transforming activities.

Body:

DU-145, PC-3, and LanCaP cell lines were purchased from the Americal Type Culture Collection, and passaged in tissue culture. Total RNA was extracted from exponentially growing cells and purified by guanidinium isothiocyanate acid phenol extraction (1). Comparable yields and purity were ascertained by absorption of ultraviolet light (see Table 1). As described in the Methods section of the reprint included in the Appendix, equal quantities of total mRNA from each line was mixed together. Poly A+ mRNA in the mixture of total RNA was purified by two passages over oligo dT cellulose, quantified by absorption of ultraviolet light, and stored at −70C.

Table 1: Preparation of mRNA from prostate cancer cell lines.

Cell line	RNA yield (μg/ml)	Optical density (260nm/280nm)
LNCaP	197	2.02
DU145	79.4	1.98
PC-3	150	1.97

A cDNA synthesis kit was purchased from Stratagene (La Jolla, CA) and used to prepare first strand and second strand cDNA using a trace amount of radiolabel to facilitate visualization of the final product. Gel electrophoresis of this cDNA indicated a low final yield of cDNA, as determined by ethidium bromide staining and autoradiography of the dried gel. Rather than perform the screen using sub-optimal yields of cDNA we elected to repeat the RNA extraction, poly A+ mRNA isolation, and cDNA synthesis. This work is in progress at the time of the annual report and the screen will be completed this year. Increased effort by the principal investigator as requested and approved will facilitate completion of the work.

At the same time, several studies indirectly related to the proposal were successfully completed. To test whether novel oncogenes identified using the RK3E assay are activated in vivo, we worked out the technique of mRNA in situ hybridization and used the assay to analyze expression of GKLF in oral squamous dysplasia and

carcinoma. As shown on the cover of the June issue of Cell Growth and Differentiation, GKLF expression is prominently increased in dysplastic oral epithelium. This result supports the validity of the expression cloning assay and suggests that GKLF or novel oncogenes may likewise be activated in epithelial neoplastic lesions such as prostatic intraepithelial neoplasia (PIN) and invasive carcinoma.

Initial mRNA in situ hybridization assays of GKLF expression in paraffin-embedded PIN and prostatic tumors suggested that GKLF is likewise expressed in this tumor type. A novel monoclonal antibody specifically detects GKLF by western blot and by immunocytochemistry of tissue culture cells. Immunohistochemical studies currently in progress will be used to detect the protein in normal, neoplastic PIN, and invasive prostatic lesions to determine the temporal relationship of GKLF expression and tumor progression. If GKLF can be detected in normal prostatic epithelium and/or tumor, we would like to include these expression studies as additions to the original statement of work upon approval by the Grants Officer.

Key Research Accomplishments:
- Culture and passage of prostate cancer cell lines
- Preparation of total mRNA
- Isolation of polyA+ mRNA
- Synthesis of cDNA
- Validation of the RK3E assay by showing that GKLF is an oncogene activated during carcinoma progression in vivo
- Development of an immunocytochemical assay for GKLF polypeptide

Reportable outcomes:
Provisional patent application, May 19, 1999: Oncogene Identification by Transformation of RK3E cells and uses thereof; D6236

Conclusions: The ability to identify the major transforming oncogenes activated in epithelial-derived tumors is critical to the understanding carcinoma pathogenesis. The RK3E assay showed that transformation of epithelial cells in vitro is a highly specific assay that does not lead to identification of artifacts such as truncated cDNAs or cDNAs that are irrelevant to tumor progression in vivo. Identification of GKLF as an oncogene indicates that the major transforming activities in tumors remain poorly characterized. Application of the assay to poorly understood tumors such as prostate cancer will lead to better insight into pathogenesis.

References:

1. Chomczynski, P. and Sacchi, N. Single-step method of RNA isolation by acid guanidinium thiocyanate-phenol-chloroform extraction. Anal. Biochem., *162*: 156-159, 1987.

Appendices:

1. Reprint of Foster et al.

Bibliography: none

Personnel:
Persons receiving pay from the research effort include research assistant P. McKie-Bell, and principal investigator J. Michael Ruppert. Graduate student W. Foster is paid by the Division of Hematology-Oncology as part of a matching agreement with the Army.

Appendix DAMD17-98-1-8570

Oncogene Expression Cloning by Retroviral Transduction of Adenovirus E1A-immortalized Rat Kidney RK3E Cells: Transformation of a Host with Epithelial Features by c-MYC and the Zinc Finger Protein GKLF[1]

K. Wade Foster, Songrong Ren,[2] Iuri D. Louro, Susan M. Lobo-Ruppert, Peggy McKie-Bell, William Grizzle, Martha R. Hayes, Thomas R. Broker, Louise T. Chow, and J. Michael Ruppert[3]

Department of Biochemistry and Molecular Genetics [K. W. F., S. R., I. D. L., S. M. L-R., M. R. H., T. R. B., L. T. C., J. M. R.], Division of Hematology/Oncology, Department of Medicine [P. M-B., J. M. R.], Department of Pathology [W. G.], and Oral Cancer Research Center and Comprehensive Cancer Center [W. G., T. R. B., L. T. C., J. M. R.], University of Alabama at Birmingham, Birmingham, Alabama 35294-3300

Abstract

The function of several known oncogenes is restricted to specific host cells *in vitro*, suggesting that new genes may be identified by using alternate hosts. RK3E cells exhibit characteristics of epithelia and are susceptible to transformation by the G protein RAS and the zinc finger protein GLI. Expression cloning identified the major transforming activities in squamous cell carcinoma cell lines as c-MYC and the zinc finger protein gut-enriched Krüppel-like factor (GKLF)/epithelial zinc finger. In oral squamous epithelium, *GKLF* expression was detected in the upper, differentiating cell layers. In dysplastic epithelium, expression was prominently increased and was detected diffusely throughout the entire epithelium, indicating that *GKLF* is misexpressed in the basal compartment early during tumor progression. The results demonstrate transformation of epithelioid cells to be a sensitive and specific assay for oncogenes activated during tumorigenesis *in vivo*, and identify *GKLF* as an oncogene that may function as a regulator of proliferation or differentiation in epithelia.

Introduction

Cellular oncogenes have been isolated by characterization of transforming retroviruses from animal tumors, by examination of the breakpoints resulting from chromosomal translocation, by expression cloning of tumor DNA molecules using mesenchymal cells such as NIH3T3, and by other methods (1–5). Several human tumor-types exhibit loss-of-function mutations in a tumor suppressor gene that lead to activation of a specific oncogene in a large proportion of tumors. For example, *c-MYC* expression is regulated by the *APC* colorectal tumor suppressor; expression of *GLI* is activated by loss-of-function of *PATCHED1* in human basal cell carcinoma and in animal models; E2F is activated by loss-of-function of the retinoblastoma susceptibility protein p105^{Rb}; and RAS GTPase activity is regulated by the familial neurofibromatosis gene *NF1* (6–12). The comparative genomic hybridization assay and related methods have shown that numerous uncharacterized loci in tumors undergo gene amplification (13). These observations, and the infrequent genetic alteration of known oncogenes in certain tumor types, suggest that novel transforming oncogenes remain to be identified.

One limitation to the isolation of oncogenes has been the paucity of *in vitro* assays for functional expression cloning. Whereas most studies have used NIH3T3 or other mesenchymal cells as host for analysis of oncogenes relevant to carcinoma, the potential use of a host cell with epithelial characteristics has been discussed (2). In addition, several known oncogenes exhibit cell-type specificity. *GLI*, *BCR-ABL*, *NOTCH1/TAN1*, and the G protein GIP2 have been found to transform immortalized rat cells (14–18), but not NIHT3 cells, demonstrating the potential use of alternate assays for oncogene expression cloning.

A consistent feature of human tumors is inactivation of the G$_1$ phase cell cycle regulatory pathway that includes p105^{Rb} (19–22). Loss-of-function mutations affect p105^{Rb} or the cyclin-dependent kinase inhibitors, or gain-of-function mutations occur in cyclin-dependent kinases or associated cyclins. Such alterations are rate-limiting for tumor formation *in vivo* because inheritance of these defects predisposes to retinoblastoma, cutaneous malignant melanoma, and other tumors. During viral infection of normal cells, disruption of the same pathway is critical for successful induction of the cellular DNA replicative machinery to support viral replication. Therefore, viruses express proteins, such as adenovirus E1A, that affect cell cycle progression through direct interaction with cell cycle regulators including p105^{Rb}, p27^{Kip1}, and others (23–26).

Fig. 1. RK3E cells exhibit characteristics of epithelial cells. A, confluent RK3E cells in a culture dish were fixed and stained with uranyl acetate and lead citrate, and ultra-thin sections were examined using a Hitachi 7000 transmission electron microscope. The upper surface was exposed to growth media, and the lower surface was adherent. Electron dense aggregates typical of adherens junctions (*arrows*) and desmosomes (*circled*) are shown. *Bars*, 3.2 μm (*top*) or 1.3 μm (*bottom*). B, Northern blot analysis of RK3E cells (*Lane 1*) and REF52 fibroblasts (*Lane 2*). The filter was hybridized sequentially to a desmoplakin probe (*top*) and then to β-tubulin (*bottom*). C, vimentin expression by immunocytochemistry in RK3E (*top*) and REF52 (*bottom*) cells. *Bars*, 100 μm.

Table 1 Assessment of cDNA libraries

Library	λ titer	cDNA size (N,R)[a]	Probe[b]	cDNA clones transduced[c]	Transduced RK3E cells[d]	Foci identified
Squamous cell carcinoma	8.9×10^6	1.69 (10, 1.00–3.60)	NT	$\sim 4 \times 10^6$	$\sim 1.2 \times 10^7$	13
Breast carcinoma	7.4×10^6	1.64 (18, 0.50–2.7)	hBRF	$\sim 4 \times 10^6$	$\sim 1.2 \times 10^7$	1

[a] The mean size of cDNAs in kb pairs; the number of clones sized by gel electrophoresis (N) and the size range (R) are indicated.
[b] Plaques (420,000) were analyzed by hybridization to the 5' end of the RNA polymerase III transcription factor hBRF cDNA (see "Results"); NT, not tested.
[c] The number of clones processed at each step of library construction was equal to or greater than 4×10^6. The *Bst* XI adapter strategy generates recombinant cDNA expression plasmids in an orientation-independent fashion, such that both sense and antisense vectors result.
[d] The number of RK3E cells transduced was estimated as the product of the transduction frequency (20%), the number of dishes screened (20), and the number of cells/dish (3×10^6).

We previously developed and used RK3E cells, immortalized by *E1A*, to demonstrate the transforming activity of *GLI* (17). We now show that these cells exhibit multiple features of epithelia and detect known and novel transforming activities in tumor cell lines. The epithelial features of the cells and/or the mechanism of immortalization may explain the surprising sensitivity and specificity of the assay compared with previous expression cloning approaches (27). Three of the four genes known to transform RK3E cells are activated by genetic alterations in carcinomas, and, of these genes, only *RAS* exhibits transforming activity in the commonly used host NIH3T3. We identify *GKLF*[4] (3) as an oncogene that is expressed in the differentiating compartment of epithelium and misexpressed in dysplastic epithelium. We also suggest that *GKLF* may regulate the rate of differentiation and maturation and the overall cellular transit time through epithelium. The functional similarities shared with other oncogenes, including *GLI* or *c-MYC*, identify *GKLF* as an attractive candidate gene relevant to tumor pathogenesis.

Results

RK3E Cells Have Characteristics of Epithelia.
RK3E cells are a clone of primary rat kidney cells immortalized by transfection with adenovirus *E1A in vitro* (17). The cells exhibit morphological and molecular features that are epithelioid. They are contact-inhibited at confluence and are polarized with apical and basolateral surfaces and electron-dense intercellular junctions typical of adherens junctions and desmosomes (Fig. 1A). Northern blot analysis showed that RK3E cells, but not REF52 fibroblasts, expressed desmoplakin, a major component of desmosomes and an epithelial marker (Fig. 1B). By immunocytochemical staining, the mesenchymal marker vimentin was low or undetectable in RK3E cells, but was strongly positive in REF52 cells (Fig. 1C). Neither line reacted strongly with anticytokeratin or antidesmin antibodies. These results are consistent with the observation that E1A induces multiple epithelial characteristics without inducing cytokeratin expression (28).

Karyotype analysis revealed RK3E cells to be diploid with a slightly elongated chromosome 5q as the only apparent abnormality (17). Importantly, RK3E cells can be transformed by functionally diverse oncogenes such as *RAS* and *GLI*.

[4] The abbreviations used are: GKLF, gut-enriched Krüppel-like factor; β-gal, β-galactosidase; UTR, untranslated region; MMLV, Moloney murine leukemia virus; GAPDH, glyceraldehyde-3-phosphate dehydrogenase; ISH, *in situ* hybridization.

Four such transformed lines were each homogeneous for DNA content, as determined by fluorescence analysis of propidium iodide-stained cells derived from *RAS*- (one line) or *GLI*- (three lines) induced foci, indicative of a relatively stable genetic constitution (data not shown). These properties suggested that RK3E cells may serve as an *in vitro* model for identification and mechanistic analysis of gene products involved in the progression from normal epithelial tissue to malignancy.

cDNA Library Construction. To identify transforming genes, we used mRNA from human squamous cell carcinoma- or breast tumor-derived cell lines. These tumor types do not exhibit frequent alteration of *RAS* or *GLI*. After pooling mRNAs for each tumor type, oligo dT-primed cDNA libraries were constructed in bacteriophage λ (Table 1). The libraries were high-titer (assessed before amplification on agar plates) with a mean insert size of 1.6–1.7 kb. The amplified breast cDNA library was further assessed by plaque screening for the transcription factor hBRF, using a probe derived from the 5' end of the protein coding region (bases 315–655, accession U75276). Each of the seven clones identified were derived from independent reverse transcripts, as determined by end sequencing, confirming that complexity of the library was maintained during amplification. The inserts ranged in size from 2.1–3.4 kb and contained the entire 3' UTR and much or all of the protein coding region intact. Three of the seven clones extended through the predicted initiator methionine codon, whereas four others were truncated further downstream. These results suggested that the library is relatively free of COOH-terminally truncated clones and contains full-length cDNAs even for relatively long mRNAs. The overall abundance of hBRF mRNA has not been determined.

Isolation of c-MYC and GKLF by Expression Cloning. The libraries were cloned into the MMLV retroviral expression plasmid pCTV1B (27), packaged in BOSC23 cells (29), and high-titer virus supernatants were applied to RK3E cells. Fourteen foci, identified at 10–20 days after transduction, were individually expanded into cell lines. Thirteen of these foci contained a single stably integrated cDNA, as indicated by PCR (Fig. 2A). Eleven of these PCR products were identified as human *c-MYC* by end-sequencing and restriction enzyme analysis. The *c-MYC* cDNA in *Lane 15* included the coding region and 193 bases of 5' UTR sequence (accession V00568). As determined by sequencing or restriction mapping, the other *c-MYC* cDNAs extended further 5' *(Lanes 1, 3, 5–7, 9–7, 13,* and *14)*, such that all of the clones contained the entire protein-coding region.
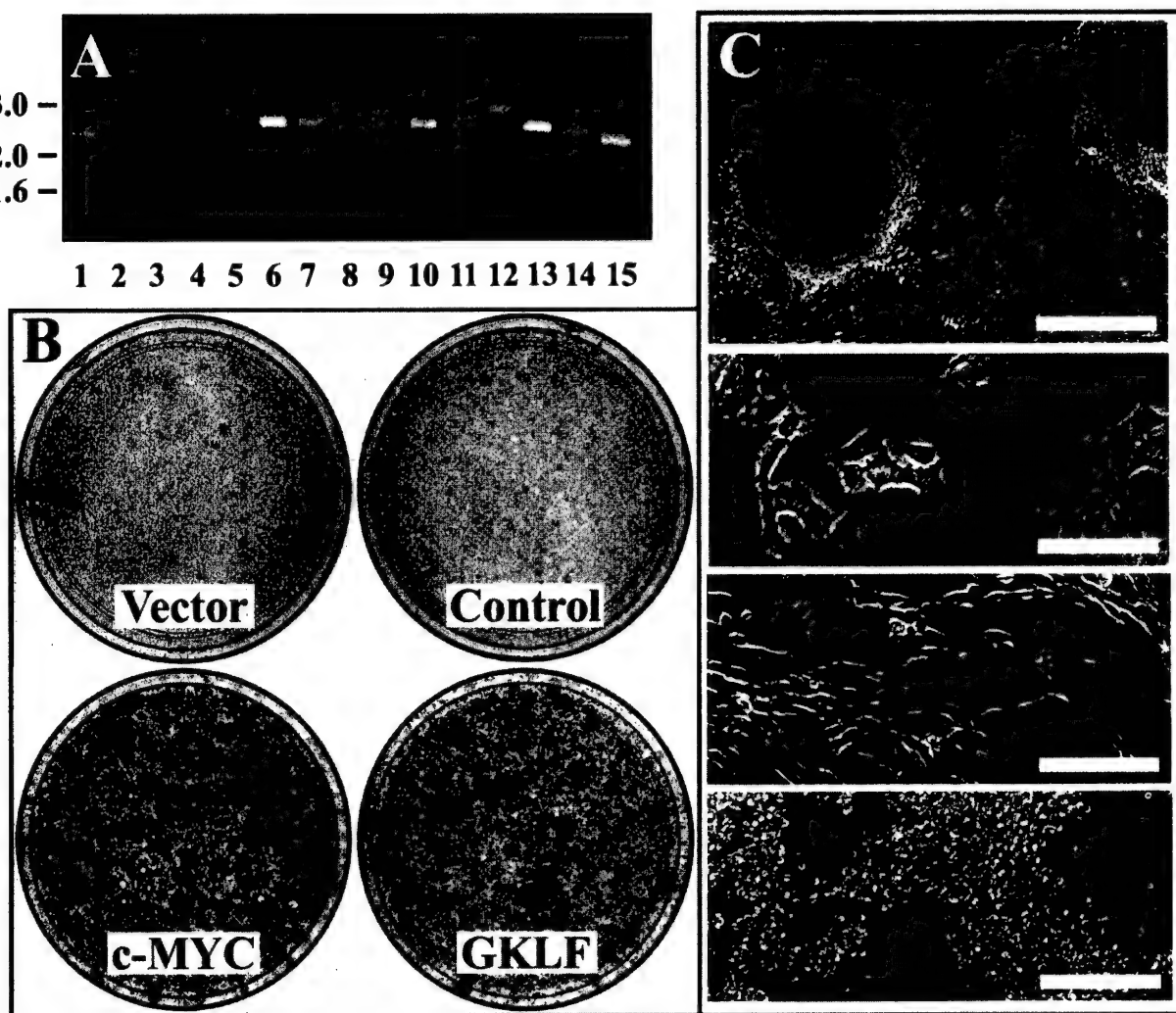
Fig. 2. Expression cloning of *c-MYC* and *GKLF*. A, identification of human cDNAs present in transformed RK3E cell lines SQC1-SQC13 (derived using a squamous cell carcinoma library, *Lanes 1* and *3–14*) and BR1 (derived using a breast carcinoma library, *Lane 15*). PCR was used in combination with vector-derived primers and cell line genomic DNA. RK3E genomic DNA served as a negative control template *(Lane 2)*. No cDNA was retrieved from cell line SQC3 *(Lane 4)*. All foci identified in the screen are represented. Molecular weight markers are indicated on the left in kb pairs. B, reconstitution of transforming activity by cloned PCR products. cDNAs were cloned into a retroviral expression plasmid, packaged into virus using BOSC23 cells, and applied to RK3E cells. Foci were fixed and stained at 3–4 weeks. *Vector*, pCTV3K; *Control*, pCTV3K-SQC1; *c-MYC*, pCTV3K-BR1; *GKLF*, pCTV3K-SQC7. C, morphology of foci and cloned cell lines. *Top to bottom: first panel*, low-power phase contrast view of adjacent foci in a dish transduced with retrovirus encoding *GKLF* (*bar*, 900 μm); *second through fourth panels*, high-power phase contrast view (*bar*, 230 μm); *second panel*, RK3E cells at subconfluence; *third panel*, *GKLF*-transformed RK3E cells; *fourth panel*, *c-MYC*-transformed RK3E cells.

In addition, two cell lines (Fig. 2*A*, *Lanes 8* and *12*) contained cDNAs coding for *GKLF*. Mouse and human *GKLF* cDNAs were previously isolated by hybridization with zinc finger consensus probes (30–32), but were not implicated as oncogenes or found to be induced during neoplastic progression. After cloning into plasmid, the sequences of these two cDNAs, termed SQC7 and SQC11, were obtained in total. As determined by comparison with multiple expressed sequence tags and two full-length coding sequence files in the database (accessions U70663 and AFO22184), each contained the predicted GKLF protein coding region bounded by 5′ and 3′ UTRs. An ATG in good context for translation initiation was located at base 330, with the predicted terminator codon at base 1740. Both isolates were

artificially truncated at the *Xho*I site in the 5′ UTR during library preparation. Because the transcripts had been processed using distinct AAUAAA polyadenylation signals, the cDNAs were slightly different in length and derived from independent mRNA molecules (Fig. 2*A*).

Sequencing revealed these two *GKLF* isolates to be identical within the residual 5′ UTR and throughout the coding region. A single bp difference in the 3′ UTR represents a PCR-induced error or a rare variant, as determined by comparison with ESTs. Comparison to a placenta-derived sequence (accession U70663) revealed three single bp differences in the coding region. These differences were resolved by alignment with other sequences in the database (accessions AF022184 and AA382289) from normal tissues, indi-

Table 2 Retroviral transduction of reconstituted *GKLF* and *c-MYC* expression vectors

Plasmid	Focus assay (no. foci/10 cm dish)[a]	Colony morphology assay (no. transformed/total)[b]
pCTV3K (vector)	0, 0	0/184
pCTV3K-SQC1[c] (*c-MYC*)	0, 0	0/232
pCTV3K-SQC5 (*c-MYC*)	>1000, >1000	ND[d]
pCTV3K-BR1 (*c-MYC*)	>1000, >1000	81/91 (89%)
pCTV3K-SQC7 (*GKLF*)	>1000, >1000	91/206 (44%)
pCTV3K-SQC11-2[e] (*GKLF*)	>1000, >1000	ND
pCTV3K-SQC11-3 (*GKLF*)	>1000, >1000	ND

[a] RK3E cells were transduced with 4 ml of virus supernatant after calcium phosphate-mediated plasmid transfection of virus packaging cells.
[b] RK3E cells were transduced with 0.4 ml of thawed viral supernatant. Cells were split 1:4 into selective media 30 h later. At 2 weeks, drug-resistant colonies were fixed, stained, and examined visually for morphological transformation. Numbers indicate colonies/10-cm dish. A duplicate transduction experiment yielded similar results (data not shown). No colonies formed in control dishes that were not exposed to virus.
[c] pCTV3K-SQC1 is a *c-MYC* allele obtained by PCR that exhibited greatly reduced transforming activity compared with other alleles.
[d] ND, not determined.
[e] SQC11-2 and -3 are independent plasmid clones derived from the same PCR reaction (Fig 2A, *Lane 12*).

cating that the *GKLF* molecules obtained by expression cloning are predicted to encode the wild-type protein.

Reconstitution of Transforming Activity for *c-MYC* and *GKLF*. To demonstrate transforming activity, three independent PCR products each for the *c-MYC* and *GKLF* cDNAs were cloned into the retroviral expression vector pCTV3K (27), packaged into virions, and tested for transformation of RK3E cells *in vitro* (Fig. 2, *B* and *C*; Table 2). One of the *c-MYC* clones (pCTV3K-SQC1) possessed greatly reduced transforming activity in multiple experiments despite similar viral titers, as determined by induction of hygromycin resistance, suggesting that an error may have been introduced during PCR. Each of the other virus supernatants carrying *GKLF* and *c-MYC* transgenes induced >1000 foci/ dish compared with no foci for virus controls.

To determine the efficiency of transformation by *GKLF* and *c-MYC*, a colony morphology assay was used, as described previously (27). Virally transduced cells were selected in hygromycin at low confluence, and stable colonies were fixed, stained, and scored for morphological transformation by visual inspection as above for foci (Table 2). The *c-MYC*-transduced cells exhibited loss of contact inhibition and dense growth in 89% of colonies. The *GKLF*-transduced cells exhibited a transformed morphology in 44% of colonies. In comparison, a previous study showed that 70% and 40% of NIH3T3 colonies transduced by viruses carrying *RAS* and *RAF* exhibited a transformed morphology (27). We, likewise, tested virus supernatants for transformation of NIH3T3 cells. Neither *c-MYC* nor *GKLF* induced morphological transformation of NIH3T3 colonies, as previously described for *GLI* and others (data not shown; Ref. 17). These results identify the RK3E assay as not only highly specific, but also sensitive to the activity of a select group of oncogenes.

In lieu of sequencing the *c-MYC* alleles, we confirmed that wild-type *c-MYC* can transform RK3E cells. A human wild-type expression vector (pSRαMSV *c-MYC* tk-neo) induced foci using direct plasmid transfection of RK3E cells in multiple experiments. Foci were observed at a similar frequency using known wild-type or new *c-MYC* isolates when analyzed in parallel (data not shown). In addition, retrovirus encoding the estrogen receptor-c-MYC (wild-type) fusion protein induced morphological transformation of RK3E cells in

the presence or absence of 4-hydroxy-tamoxifen (33). No effect was observed for controls (empty vector or a control containing a deletion in c-MYC residues 106–143).

Northern blot analysis of transformed RK3E cell lines demonstrated expression of the *c-MYC* and *GKLF* vector-derived transcripts (Fig. 3A). No endogenous transcripts were detected at the stringency used in this experiment. Compared with RK3E cells at subconfluence (*Lane 1*) or confluence (*Lane 2*), no consistent increase of *E1A* transcripts was detected in cells transformed by *RAS*, *GLI*, *c-MYC*, or *GKLF*, suggesting that these genes act upon cellular targets to induce transformation.

To detect the endogenous rat *GKLF* transcript, we used reduced-stringency wash conditions and a *Sma*I fragment from the coding region exclusive of the COOH-terminal zinc fingers and with no sequence similarity to other genes in the database. By this approach, the apparent *GKLF* transcript was identified and migrated at 3.1 kb, similar to the human 3.0-kb transcript, in RK3E and all derivative-transformed cell lines (data not shown). A single transcript with the same mobility was detected by hybridization of the filter to fulllength coding region probe. These studies revealed similar *GKLF* expression in RK3E and in derivatives transformed by *RAS*, *GLI*, or *c-MYC*. The results show that *GKLF* mRNA expression is not significantly altered by these other oncogenes and is consistent with function of *GKLF* in an independent pathway.

Cell lines derived from foci induced by *c-MYC* or *GKLF* were further tested for tumorigenicity in athymic mice by s.c. inoculation at four sites for each line (Table 3; Ref. 17). Tumors were >1 cm in diameter and were scored at 2–4 weeks after inoculation. Cells transformed by *c-MYC* induced tumors in 75% or 100% of sites injected (two lines tested). Three lines transformed by *GKLF* each induced tumors in 50–75% of sites injected. No tumors resulted from injection of RK3E cells, whereas a *GLI*-transformed cell line induced tumors in each of the four sites injected. In all, *GKLF* cell lines induced tumors in 8 of 12 injection sites, compared with 7 of 8 injection sites for *c-MYC* and 4 of 4 injection sites for *GLI*. *GKLF*-induced tumors also grew more slowly *in vivo*, reaching 1 cm in diameter by 3.4 weeks, on average, compared with 2.6 weeks for c-MYC and 3 weeks for *GLI*. The
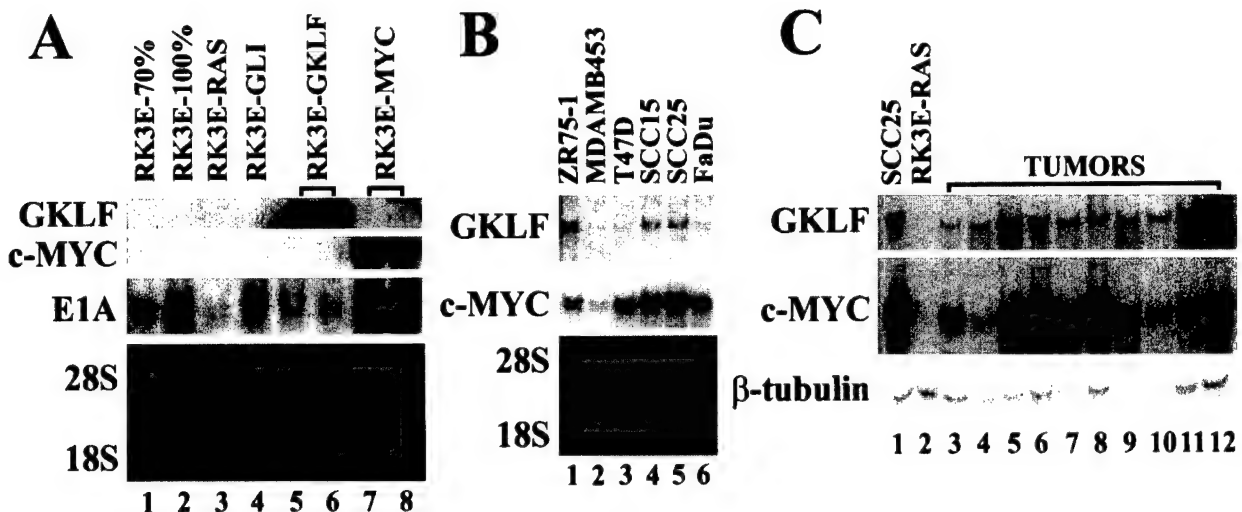
Fig. 3.   Northern blot analysis of c-MYC and GKLF expression. Total RNA (25 μg) was loaded for each sample. A, analysis of transgene expression in RK3E cells and derivative cell lines transformed by the indicated oncogene. Lane 1, RK3E cells in exponential growth phase; Lane 2, RK3E cells incubated at confluence for 5 days. Ethidium bromide-stained RNA is shown below after transfer to the filter. B, endogenous GKLF (3.0 kb) or c-MYC (2.3 kb) expression in tumor cell lines. Lanes 1–3, breast cancer lines; Lanes 4–6, squamous cell carcinoma lines. C, analysis of gene expression in laryngeal squamous cell carcinoma. Lane 1, SCC25 cell line; Lanes 3–6, 9, and 12, primary tumors; Lanes 7, 8, 10, and 11, metastatic tumors; Lanes 3–12 correspond to case numbers 5, 8, 18–20, 6, and 21–24, respectively (see Table 4). RK3E-RAS cell RNA served as a negative control (Lane 2), whereas hybridization to β-tubulin served as a control for loading.

Table 3   Tumorigenicity of RK3E-derived cell lines in athymic mice

Cell line	No. tumors/ no. sites injected	Tumor latency in vivo (weeks)[a]	Doubling time in vitro (h)
RK3E	0/4	–	12.7
RK3E-c-MYC BR1[b]	3/4	3,3,4	19.1
RK3E-c-MYC B[c]	4/4	2,2,2,2	19.8
RK3E-GKLF E	3/4	3,3,3	33.7
RK3E-GKLF F	2/4	4,4	27.0
RK3E-GKLF G	3/4	3,3,4	ND[d]
RK3E-GLI	4/4	3,3,3,3	18.0

[a] The time required for tumors to reach 1 cm in diameter is indicated.
[b] Cell line derived from a focus identified in the original screen using a breast cancer cDNA library.
[c] Cell line derived by transformation with the reconstituted plasmid pCTV3K-BR1.
[d] ND, not determined.

moderately increased latency and decreased efficiency of tumor formation for GKLF cell lines may be attributable to the intrinsic rate of proliferation for these cells (Table 3). Although c-MYC, GLI, and GKLF cell lines all exhibited prolonged doubling times in vitro compared with RK3E cells, GKLF cells divided more slowly than the other transformed cell lines.

Northern Blot Analysis of Tumors and Tumor-derived Cell Lines. We then examined human tumors and cell lines by Northern blot analysis of total RNA (Fig. 3, B and C). GKLF expression in breast or squamous cell carcinoma cell lines was variable, with increased expression in the breast tumor line ZR75-1 and the squamous cell lines SCC15 and SCC25 (Fig. 3B). In human squamous cell carcinomas microdissected to enrich for tumor cells, GKLF expression was detected in each of 10 primary or metastatic tumors analyzed, with expression levels comparable with that for the cell line

SCC25 (Fig. 3C). The results suggest that GKLF represents a potent transforming activity that is consistently expressed in tumors as well as in tumor-derived cell lines. Because GKLF was isolated from cell lines that express the gene at a level found in tumors in vivo, the results suggest that GKLF may represent a major transforming activity in tumors, as well as in cell lines.

Gene Copy Number of c-MYC and GKLF. c-MYC was previously shown to be activated by gene amplification in ~10% of oral squamous cancers and may be activated in these or other tumors by genetic alteration of WNT-APC-β-catenin pathway components (6, 34–37). To determine whether expression of GKLF in cell lines and tumors is, likewise, associated with gene amplification, we performed Southern blot analysis (Fig. 4, A and B). Filters were sequentially hybridized to GKLF, c-MYC, and β-tubulin. Increased copies of c-MYC were identified in two cell lines used for library construction, FaDu and MCF7. Increased hybridization to c-MYC was, likewise, observed for 1 of 11 oral squamous cell carcinomas (Fig. 4A, Lane 10) and for one of nine breast carcinomas (Fig. 4B, Lane 8). These results are consistent with the published frequencies of c-MYC amplification for these tumor types (34, 35, 38). No copy number gains of GKLF were observed, indicating that other mechanisms may contribute to expression of GKLF in tumors. The same may be true for c-MYC because gene amplification in FaDu cells was associated with reduced expression compared with other oral cancer cell lines (Fig. 3B).

GKLF Expression Is Activated Early during Tumor Progression in Vivo. Previously, expression of c-MYC was found to be up-regulated consistently in dysplastic oral mucosa and in squamous cell carcinomas, and tumors with the highest levels of c-MYC expression were associated with the
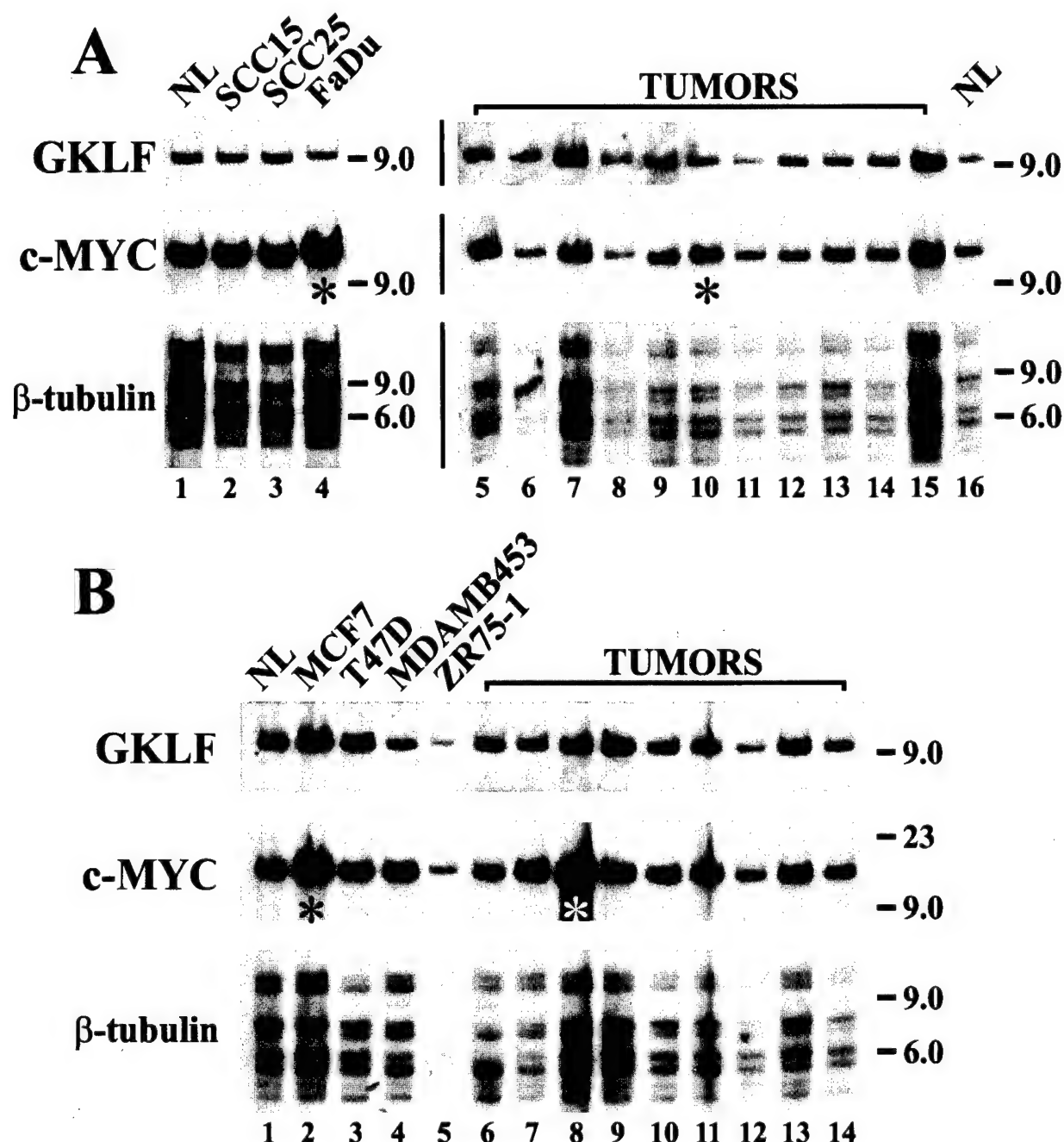
Fig. 4.   Southern blot analysis of cell line- and tumor-derived genomic DNA. DNA (5 μg) was digested with EcoRI and separated by gel electrophoresis. The filters were hybridized sequentially to GKLF, c-MYC, and β-tubulin probes. *, samples with increased apparent copy number of c-MYC. Molecular weight markers are indicated on the *right*. *NL*, normal human lymphocyte DNA. *A*, oropharyngeal squamous cell carcinoma. Cell lines *(Lanes 2–4)* and tumors *(Lanes 5–15)* are shown. *B*, breast carcinoma. Cell lines *(Lanes 2–5)* and tumors *(Lanes 6–14)* are shown.

poorest clinical outcome (36, 39–41). To determine how *GKLF* mRNA expression is altered during tumor progression, we analyzed squamous cell carcinoma of the larynx and adjacent uninvolved epithelium from the same tissue blocks using ^{35}S-labeled riboprobes by ISH analysis. In apparently normal epithelium, *GKLF* expression was detected in the spinous layer above the basal and parabasal cells (nine specimens analyzed; Fig. 5, *A-C, G-I*; Table 4). No specific *GKLF* expression was detected in the basal or parabasal cells or in the underlying dermis. In contrast, a sense control probe produced grains at a much-reduced frequency in a uniform fashion across the epithelium. *GAPDH* expression served as a positive control and was detected diffusely throughout the entire epithelium (data not shown). The ob-
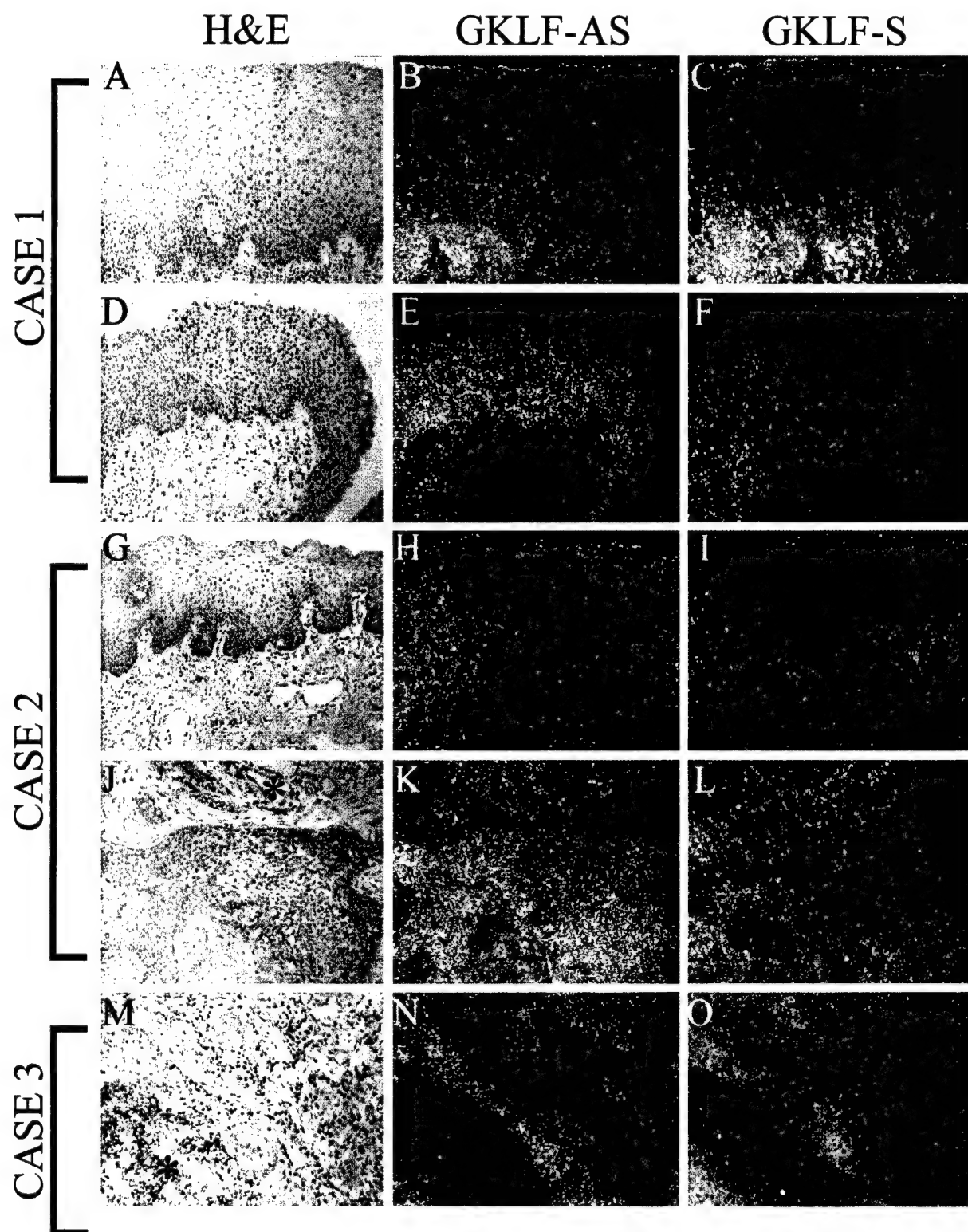
Fig. 5. ISH analysis of *GKLF*. Paraffin-embedded (*A-L*) or fresh-frozen (*M-O*) tissues were analyzed using antisense (*GKLF-AS*) or sense (*GKLF-S*) ^{35}S-labeled RNA probes. Each image (*A-O*) is 650 μm × 530 μm. Sections were stained with H&E. *Case 1*, *A-C*, uninvolved epithelium in a patient with primary laryngeal squamous cell carcinoma; *D-F*, adjacent dysplastic epithelium within the same tissue block. *Case 2*, *G-I*, uninvolved epithelium; *J-L*, adjacent primary tumor nests within stroma in the same tissue block; ∗, a salivary gland and ducts. *Case 3*, *M-O*, metastatic laryngeal squamous cell carcinoma infiltrating a lymph node; ∗, lymphocytes.

Table 4 Expression of *GKLF* in oral epithelium and tumors

Case[a]	Histopathology (U,[b]D,P,M)	Tissue source (PE/FF)	Method (N/ISH)	GKLF expression
1	U,D,P	PE	ISH	D,P>U
2	U,D	PE	ISH	D>U
2	U,P	PE	ISH	P>U
3	M	FF	ISH	+
4	U,D	PE	ISH	D>U
5	P	FF	N,ISH	+
6	M	FF	N,ISH	+
7	P	FF	ISH	+
8	P	FF	N,ISH	+
9	D,P	PE	ISH	D,P+
10	M	PE	ISH	+
11	U,D,P	PE	ISH	D,P>U
12	U,D	PE	ISH	D>U
12	U,D,P	PE	ISH	D,P>U
13	U	PE	ISH	+
13	P	PE	ISH	+
14	P	PE	ISH	+
14	M	PE	ISH	+
15	D	PE	ISH	+
15	D	PE	ISH	+
15	D,P	PE	ISH	D,P+
16	U,D,P	PE	ISH	D,P>U
16	M	PE	ISH	+
17	D,P	PE	ISH	D,P+
18	P	FF	N	+
19	P	FF	N	+
20	M	FF	N	+
21	P	FF	N	+
22	M	FF	N	+
23	M	FF	N	+
24	P	FF	N	+

[a] Each row corresponds to a tissue specimen. Levels of gene expression indicate changes identified within, rather than between, single tissue sections. For some cases, multiple specimens isolated during the same surgical procedure were analyzed. ISH results were confirmed by analysis of sections in duplicate.
[b] U, uninvolved or normal-appearing epithelium; D, dysplastic epithelium; P, primary tumor; M, metastatic tumor; PE, paraffin-embedded; FF, fresh-frozen; N, Northern; D,P>U, increased expression in dysplasia and primary tumor compared with uninvolved epithelium in the same section; D,P+, expression in both dysplasia and adjacent primary tumor.

served pattern of *GKLF* expression is identical to the pattern in normal mouse skin (32).

For each of 12 specimens analyzed, dysplastic epithelium exhibited increased *GKLF* expression throughout the epithelium (Fig. 5, *D-F*; Table 4, *Cases 1, 2, 4, 9, 11, 12,* and *15–17*). In contrast to results obtained in normal-appearing epithelium, there was no reduction of expression in the basal and parabasal layers compared with superficial layers. For tissue sections that contained both uninvolved epithelium and adjacent dysplastic epithelium, the overall level of *GKLF* expression in dysplastic epithelium was prominently elevated compared with the *GKLF*-positive cell layers in uninvolved epithelium (Fig. 5, *B, E,* and *H*; Table 4, *Cases 1, 2, 4, 11, 12,* and *16*). These results suggest that *GKLF* expression is qualitatively and quantitatively altered in dysplasia, that exclusion of *GKLF* from the basal and parabasal cell layers is lost early during neoplastic progression, and that *GKLF* exhibits properties of an oncogene not only *in vitro*, but also *in vivo*.

As shown by Northern blot analysis, *GKLF* transcripts are consistently present in tumor-derived mRNA (Fig. 3C; Table 4). To determine whether *GKLF* is expressed in tumor cells, we examined laryngeal squamous cell carcinomas by mRNA ISH. Expression was detected in each primary (13 cases) or metastatic (5 cases) tumor examined (Fig. 5, *J-O*; Table 4), with all or nearly all tumor cells associated with silver grains. The level of expression was somewhat heterogeneous, with higher levels found in the periphery and in nodules of tumor containing centrally necrotic cells or keratin pearls. As for dysplastic epithelium, expression in tumor cells was consistently elevated compared with uninvolved epithelium in the same sections (Fig. 5, *H* and *K*; Table 4, *Cases 1, 2, 11, 12,* and *16*). However, expression in tumor cells was not higher than in dysplastic epithelium (*Cases 1, 9, 11, 12,* and *15–17*). For several cases, expression in the most dysplastic epithelium was higher than in adjacent *GKLF*-positive tumor, suggesting that *GKLF* expression is specifically activated during the transition from normal epithelium to dysplasia, before invasion or metastasis.

Discussion

The results demonstrate that cells with an epithelial phenotype can be used for identification of transforming activities present in carcinoma-derived cell lines. The assay repeatedly identified two genes, and none of the isolated cDNAs were artificially truncated or rearranged within the protein coding region. This indicates that transformation of these cells is unusually specific to a few pathways or genes, including *c-MYC*, *GKLF*, *RAS*, and *GLI*. *c-MYC*, *RAS*, and *GLI* are directly or indirectly activated by genetic alterations in diverse carcinoma types during tumor progression *in vivo* (9, 10, 42–44). For both breast and oral squamous carcinoma, the tumor types analyzed in this study, *c-MYC* gene amplification is one of the more frequent oncogene genetic alterations and is observed in 10–15% of cases. By analogy, novel oncogenes identified by the RK3E assay may be directly activated in neoplasms through gain-of-function mutations or indirectly activated by loss-of-function genetic alterations.

Whitehead *et al.* (27) developed the retroviral vectors that we used in this study for transduction of NIH3T3 cells, in which they isolated 19 different cDNAs encoding 14 different proteins. Known oncogenes were isolated, including *raf-1*, *lck*, and *ect2*. Other known genes included phospholipase C-γ_2, β-catenin, and the thrombin receptor. In addition to the known genes, seven novel cDNAs were isolated, including several members of the CDC24 family of guanine nucleotide exchange factors. Only the thrombin receptor was isolated more than once, and many of the 14 different genes identified were truncated within the protein coding region. The diversity of cDNAs isolated in the NIH3T3 assay is in contrast to results obtained in the current study. The specificity of the RK3E assay may be attributable to the "tumor suppressor" activity of the *E1A* oncogene (28, 45). Although *E1A* antagonizes p105^{Rb} and immortalizes primary cells, it also induces epithelial differentiation in diverse tumor types, including sarcoma, and suppresses the malignant behavior of tumor cells *in vivo*.

GKLF was previously isolated by hybridization to zinc finger probes (30–32). The human gene is located at chromo-

some 9q31 and is closely linked to the autosomal dominant syndrome of multiple self-healing squamous epitheliomata (31, 32, 46, 47). Affected individuals develop recurrent invasive, but well-differentiated, tumors morphologically similar to squamous carcinoma that spontaneously regress. Although *GKLF* has been proposed as a candidate tumor suppressor gene relevant to multiple self-healing squamous epitheliomata (32), our results suggest that activating mutations could account for the syndrome.

GKLF encodes a nuclear protein that functions as a transcription factor when bound to a minimal essential binding site of $5'-^G/_A{}^G/_AGG^C/_TG^C/_T-3'$ (48). The 470 residue polypeptide exhibits modular domains that mediate nuclear localization, DNA binding, and transcriptional activation or repression (31, 32, 49, 50). In mice, *GKLF* expression is found predominately in barrier epithelia, including mucosa of the mouth, pharynx, lung, esophagus, and small and large intestine (30, 32). A role for *GKLF* in differentiation or growth arrest was suggested by the onset of expression at the time of epithelial differentiation (approximately embryonic day 13; Refs. 32 and 51) and by similarity within the zinc finger domain to family members erythroid Krüppel-like factor and lung Krüppel-like factor that were previously associated with growth-arrest or differentiation-specific gene expression (52, 53). Similarity to these other genes is limited to the DNA-binding zinc finger region.

Our results show that *GKLF* can induce proliferation when overexpressed *in vitro*. Analysis of expression in dysplastic cells and tumor cells *in vivo* provides independent evidence that *GKLF* exhibits properties expected of an oncogene. Genetic progression of carcinoma seems to involve genes and pathways important for homeostasis of normal epithelium (6, 7, 9, 54). For example, the zinc finger protein GLI is expressed in normal hair shaft keratinocytes, whereas *c-MYC* is expressed in normal epithelium of the colonic mucosa. In tumors derived from these tissues, *GLI* and *c-MYC* are more frequently activated by recessive genetic changes in upstream components of their respective biochemical pathways than by gain-of-function alterations such as gene amplification. Up-regulation of *GKLF* expression in dysplastic epithelium and tumor cells *in vivo* is particularly interesting as expression seems not to be increased by proliferation *in vitro*. Expression of the endogenous *GKLF* mRNA in RK3E cells was similar in cycling *versus* contact-inhibited cells (data not shown). In contrast, *GKLF* is significantly induced in NIH3T3 cells during growth arrest (30). These different results suggest that cell type-specific mechanisms can regulate *GKLF* expression, and that *GKLF* may play different roles in epithelial *versus* mesenchymal cells.

Squamous epithelium is divided into compartments (55, 56). In the basal cell layer, proliferative reserve or stem cells possess long-term or unlimited self-renewal capacity, whereas the parabasal transit amplifying cells undergo several rounds of mitosis and then withdraw from the cell cycle to differentiate into spinous cells that form the mid strata of the epithelium. These cells then undergo terminal differentiation and programmed cell death at the surface. Proliferation and differentiation are normally balanced such that overall cell number remains constant. In contrast to *GLI* and *c-MYC*,

GKLF expression in skin seems limited to the differentiating compartment (32). A simple model is that *GKLF* normally regulates the rate of maturation and shedding and the overall transit time for individual cells. The thickness of epithelium, which varies greatly in development and in different adult tissues, may be regulated not only by alterations in the rate of cell division in the basal layer, but also in response to *GKLF* or similarly acting molecules in the suprabasal layers. This model is consistent with the relatively late induction of *GKLF* during mouse development, and is testable by modulating expression of *GKLF* in transgenic animals or using raft epithelial cultures *in vitro*. Activation of *GKLF* in the basal layer of dysplastic epithelium suggests that dysplasia and progression to invasion and metastasis could result from loss of normal compartment-specific patterns of gene expression.

In summary, *GKLF*, *c-MYC*, and *GLI* are potent oncogenes in epithelioid RK3E cells *in vitro*, are analogous with respect to their expression in normal epithelium, and have potentially complex roles in the regulation of epithelial cell proliferation, differentiation, or apoptosis (6, 7, 9, 44, 56–58). How *GKLF* contributes to these processes will require a better understanding of its function and of the pathways that regulate *GKLF* activity in epithelia.

Materials and Methods

Immunocytochemistry. Immunocytochemical assays were performed in the Immunopathology Laboratory at The University of Alabama at Birmingham. Antibodies to vimentin and desmin were from Dako (Carpenteria, CA). A mixture of anticytokeratin included AE1/AE3 (Biogenics, San Ramon, CA), CAM5.2 (Becton Dickinson, San Jose, CA), and MAK-6 (Zymed, South San Francisco, CA). Human tissue served as a positive control for each antibody. No signal was obtained in the absence of primary antibody.

Construction of cDNA Libraries. Two cDNA libraries were constructed using the ZAP-Express cDNA synthesis kit (Stratagene, La Jolla, CA). A library was prepared from human squamous cell carcinoma cells derived from tumors of the oro-pharynx. Equal quantities of total mRNA from cell lines SCC15, SCC25, and FaDu (American Type Culture Collection, Manassas, VA) were pooled. Similarly, equal quantities of mRNA from the breast cancer cell lines MCF-7, ZR75–1, MDAMB-453, and T47D (American Type Culture Collection) were pooled. For each pool, poly(A)+ mRNA was selected by two cycles of oligo-dT cellulose affinity chromatography, and 5 μg were reverse transcribed using an oligo-dT linker primer and MMLV reverse transcriptase. Double-stranded cDNA was synthesized using *Escherichia coli* RNase H and DNA polymerase I. cDNA was ligated to λZAP EXPRESS bacteriophage arms and packaged into virions. The λ titer and the frequency of nonrecombinants were determined before amplification of the library on bacterial plates (Table 1). The frequency of nonrecombinant clones was estimated to be <2% by complementation of β-gal activity (blue/white assay). Phage were converted to pBKCMV plasmids by autoexcision in bacteria. Insert sizes in randomly selected clones were determined at this step by gel electrophoresis of plasmid DNA digested with *SaI* and *NotI* (Table 1). The pBKCMV plasmid libraries were amplified in soft agar at 1×10^4 colony forming units/ml (27). After incubation at 37°C for 15 h, bacterial cells within the agar bed were isolated by centrifugation, amplified for 3–4 doublings in culture, and plasmid DNA was purified using a Qiagen column (Qiagen, Inc., Chatsworth, CA).

To generate libraries in a retroviral expression vector, cDNA inserts were excised from 10 μg of plasmid using *SaI* and *XhoI*. After treatment with Klenow and dNTPs and extraction with phenol, the DNA was ligated to 5' phosphorylated *BstXI* adapters (5'-TCAGTTACTCAGG-3' and 5'-CCTGAGTAACTGACACA-3'), as described (27). After treatment with *NotI*, excess adapters were removed by gel filtration, and the residual vector was converted to a 9.0-kb dimer using the *NotI* site and T4 DNA

ligase. The cDNA was size-fractionated by electrophoresis in Sea Plaque agarose (FMC BioProducts, Rockland, ME) and fragments 0.6–8.5 kb were isolated and ligated to the *Bst*XI- and alkaline phosphatase-treated MMLV retroviral vector pCTV1B (27). *E. coli* MC1061/p3 were transformed by electroporation and selected in soft agar as above.

Retroviral Transduction. The libraries were analyzed in two transfection experiments performed on consecutive days. For each library, ten 10-cm dishes of BOSC23 ecotropic packaging cells at 80%–90% confluence were transfected using 30 μg of plasmid DNA/dish (29). The transfection efficiency for these cells was ~60%, as determined using a β-gal control plasmid. Viruses were collected in a volume of 9.0 ml/dish at 36–72 h after transfection, filtered, and the 9.0 ml was expressed into a 10 cm dish containing RK3E cells at ~30% confluence. Polybrene was added to a final concentration of 10 μg/ml. After 15 h, and every 3 days thereafter, the cells were fed with growth media (17). A total of 20 RK3E dishes were transduced for each library. A β-gal retroviral plasmid transduced at least 20–30% of RK3E cells in control dishes. For colony assays, hygromycin was used at 100 μg/ml. Cell proliferation rates for transformed cell lines was measured by plating 2×10^5 cells in duplicate and counting cells 96 h later using a hemacytometer (Table 3).

PCR Recovery of Proviral Inserts. PCR reactions used 200 ng of cell line genomic DNA, 20 mM Tris-HCl (pH 8.8), 87 mM potassium acetate, 1.0 mM MgCl$_2$, 8% glycerol, 2% DMSO, 0.2 mM of each dNTP, 32 pmol of each primer (5'-CCTCACTCCTTCTCTAGCTC-3'; 5'-AACAAATTGGAC-TAATCGATACG-3'; Ref. 27), 5 units of Taq polymerase (Life Technologies, Inc., Gaithersburg, MD), and 0.3 units of *Pfu* polymerase (Stratagene, La Jolla, CA) in a volume of 0.05 ml. Cycling profiles were: 95°C for 1 min; then 95°C for 10 s, 59°C for 40 s, 68°C for 8 min (35 cycles).

RNA Extraction and Northern Blot Analysis. Tumor samples were obtained through the Tissue Procurement Facility of the University of Alabama at Birmingham Comprehensive Cancer Center and the Southern Division of the Cooperative Human Tissue Network. Microdissection was used to isolate tissue composed of >70% tumor cells. Total RNA was isolated as described (59), then denatured and separated on a 1.5% formaldehyde agarose gel and transferred to nitrocellulose (Schleicher and Schuell, Keene, NH). Prehybridization was at 42°C for 3 h in 50% formamide, $4 \times$ SSC [SSC is 150 mM NaCl, 15 mM sodium citrate (pH 7.5)], 0.1 M sodium phosphate (pH 6.8), 0.1% sodium PP$_i$, 0.1% SDS, $5 \times$ Denhardt's, and 25 μg/ml denatured salmon sperm DNA. Hybridization was at 42°C for 16–20 h. The hybridization mixture contained 45% formamide, $4 \times$ SSC, 0.1 M sodium phosphate (pH 6.8), 0.075% sodium PP$_i$, 0.1% SDS, 10% dextran sulfate, and 100 μg/ml denatured salmon sperm DNA. After hybridization, the filter was washed twice in $2 \times$ SSC, 0.1% SDS for 20 min at room temperature, then washed in $0.3 \times$ SSC, 0.3% SDS for 30 min at 59°C (for detection of rat transcripts) or 65°C. For stripping of hybridized probes, the filter was placed in a solution of $2 \times$ SSC, 25 mM Tris-HCl (pH 7.5), 0.1% SDS at initial temperature of 95°C, and shaken for 10 min at room temperature.

ISH. ISHs were conducted as described (60), using sense and antisense ^{35}S-labeled riboprobes generated from a 301-bp *Eco*RI fragment derived from the *GKLF* 3' UTR positioned 40 bases from the stop codon. A *GAPDH* antisense probe corresponding to bases 366–680 (accession M33197) was synthesized using a commercially available template (Ambion, Inc., Austin, TX). All results were obtained in duplicate. High stringency washes were in $0.1 \times$ SSC and 0.1% (v/v) 2-mercaptoethanol at 58°C for *GKLF* or 68°C for *GAPDH*. Slides were coated with emulsion and exposed for 14 days.

Nucleotide Sequencing. Automated sequence analysis was performed for the two independent *GKLF* isolates using vector-derived primers and sense or antisense primers spaced at 400-bp intervals within the inserts. The complete sequence was obtained for both clones, with one of the clones analyzed for both strands. Primer sequences are available upon request. *GKLF* sequence was submitted to GenBank (accession AF105036).

References

1. Weinberg, R. A. Oncogenes, antioncogenes, and the molecular bases of multistep carcinogenesis. Cancer Res., *49:* 3713–3721, 1989.

2. Hunter, T. Cooperation between oncogenes. Cell, *64:* 249–270, 1991.

3. Bishop, J. M. Molecular themes in oncogenesis. Cell, *64:* 235–248, 1991.

4. Miki, T., and Aaronson, S. A. Isolation of oncogenes by expression cDNA cloning. Methods Enzymol., *254:* 196–206, 1995.

5. Look, A. T. Oncogenic transcription factors in the human acute leukemias. Science (Washington DC), *278:* 1059–1064, 1997.

6. He, T. C., Sparks, A. B., Rago, C., Hermeking, H., Zawel, L., da Costa, L. T., Morin, P. J., Vogelstein, B., and Kinzler, K. W. Identification of c-MYC as a target of the APC pathway. Science (Washington DC), *281:* 1509–1512, 1998.

7. Korinek, V., Barker, N., Moerer, P., van Donselaar, E., Huls, G., Peters, P. J., and Clevers, H. Depletion of epithelial stem-cell compartments in the small intestine of mice lacking TCF-4. Nat. Genet., *19:* 379–383, 1998.

8. Goodrich, L. V., Milenkovic, L., Higgins, K. M., and Scott, M. P. Altered neural cell fates and medulloblastoma in mouse patched mutants. Science (Washington DC), *277:* 1109–1113, 1997.

9. Dahmane, N., Lee, J., Robins, P., Heller, P., and Ruiz i Altaba, A. Activation of the transcription factor GLI1 and the sonic hedgehog signaling pathway in skin tumours. Nature (Lond.), *389:* 876–881, 1997.

10. Hahn, H., Wojnowski, L., Zimmer, A. M., Hall, J., Miller, G., and Zimmer, A. Rhabdomyosarcomas and radiation hypersensitivity in a mouse model of Gorlin Syndrome. Nat. Med., *4:* 619–622, 1998.

11. Xu, G. F., O'Connell, P., Viskochil, D., Cawthon, R., Robertson, M., Culver, M., Dunn, D., Stevens, J., Gesteland, R., White, R., Weiss, R. The neurofibromatosis type 1 gene encodes a protein related to GAP. Cell, *62:* 599–608, 1990.

12. Chellappan, S. P., Hiebert, S., Mudryj, M., Horowitz, J. M., and Nevins, J. R. The E2F transcription factor is a cellular target for the RB protein. Cell, *65:* 1053–1061, 1991.

13. Kallioniemi, O. P., Kallioniemi, A., Sudar, D., Rutovitz, D., Gray, J. W., Waldman, F., and Pinkel, D. Comparative genomic hybridization: a rapid new method for detecting and mapping DNA amplification in tumors. Semin. Cancer Biol., *4:* 41–46, 1993.

14. Iftner, T. G., Bierfelder, S., Csapo, Z., and Pfister, H. Involvement of human papillomavirus type 8 genes E6 and E7 in transformation and replication. J. Virol., *62:* 3655–3661, 1988.

15. Lugo, T. G., and Witte, O. N. The *BCR-ABL* oncogene transforms Rat-1 cells and cooperates with v-*myc*. Mol. Cell. Biol., *9:* 1263–1270, 1989.

16. Pace, A. M., Wong, Y. H., and Bourne, H. R. A mutant α subunit of GIP2 induces neoplastic transformation of RAT1 cells. Proc. Natl. Acad. Sci. USA, *88:* 7031–7035, 1991.

17. Ruppert, J. M., Vogelstein, B., and Kinzler, K. W. The zinc finger protein GLI transforms rodent cells in cooperation with adenovirus E1A. Mol. Cell. Biol., *11:* 1724–1728, 1991.

18. Capobianco, A. J., Zagouras, P., Blaumueller, C. M., Artavanis-Tsakonas, S., and Bishop, J. M. Neoplastic transformation by truncated alleles of human NOTCH1/TAN1 and NOTCH2. Mol. Cell. Biol., *17:* 6265–6273, 1997.

19. Draetta, G. F. Mammalian G1 cyclins. Curr. Opin. Cell Biol., *6:* 842–846, 1994.

20. Hussussian, C. J., Struewing, J. P., Goldstein, A. P., Higgins, P. A., Ally, D. S., Sheahan, M. D., Clark, W. H. J., Tucker, M. A., and Dracopoli, N. C. Germline p16 mutations in familial melanoma. Nat. Genet., *8:* 15–21, 1994.

21. Sherr, C. J., and Roberts, J. M. Inhibitors of mammalian G(1) cyclin-dependent kinases. Genes Dev., *9:* 1149–1163, 1995.

22. Weinberg, R. A. The retinoblastoma protein and cell cycle control. Cell, *81:* 323–330, 1995.

23. Bishop, J. M. Viral oncogenes. Cell, *42:* 23–38, 1985.

24. Harlow, E., and Dyson, N. Adenovirus E1a targets key regulators of cell proliferation. Cancer Surv., *12:* 161–195, 1992.

25. Nevins, J. R. Adenovirus E1a: transcription regulation and alteration of cell growth control. Curr. Top. Microbiol. Immunol., *199:* 25–32, 1995.

26. Mal, A., Poon, R. Y. C., Howe, P. H., Toyoshima, H., Hunter, T., and Harter, M. L. Inactivation of $p27^{Kip1}$ by the viral E1a oncoprotein in TGFβ-treated cells. Nature (Lond.), *380:* 262–265, 1996.

27. Whitehead, I., Kirk, H., and Kay, R. Expression cloning of oncogenes by retroviral transfer of cDNA libraries. Mol. Cell. Biol., *15:* 704–710, 1995.

28. Frisch, S. M. E1a induces the expression of epithelial characteristics. J. Cell Biol., *127:* 1085–1096, 1994.

29. Pear, W. S., Nolan, G. P., Scott, M. L., and Baltimore, D. Production of high-titer helper-free retroviruses by transient transfection. Proc. Natl. Acad. Sci. USA, *90:* 8392–8396, 1993.

30. Shields, J. M., Christy, R. J., and Yang, V. W. Identification and characterization of a gene encoding a gut-enriched Krüppel-like factor expressed during growth arrest. J. Biol. Chem., *271:* 20009–20017, 1996.

31. Yet, S. F., Mcanulty, M. M., Folta, S. C., Yen, H. W., Yoshizumi, M., Hsieh, C. M., Layne, M. D., Chin, M. T., Wang, H., Perrella, M. A., Jain, M. K., and Lee, M. E. Human EZF, a Krüppel-like zinc finger protein, is expressed in vascular endothelial cells and contains transcriptional activation and repression domains. J. Biol. Chem., *273:* 1026–1031, 1998.

32. Garrett-Sinha, L. A., Eberspaecher, H., Seldin, M. F., and de Crombrugghe, B. A gene for a novel zinc-finger protein expressed in differentiated epithelial cells and transiently in certain mesenchymal cells. J. Biol. Chem., *271:* 31384–31390, 1996.

33. Littlewood, T. D., Hancock, D. C., Danielian, P. S., Parker, M. G., and Evan, G. I. A modified oestrogen receptor ligand-binding domain as an improved switch for the regulation of heterologous proteins. Nucleic Acids Res., *23:* 1686–1690, 1995.

34. Merritt, W. D., Weissler, M. C., Turk, B. F., and Gilmer, T. M. Oncogene amplification in squamous cell carcinoma of the head and neck. Arch. Otolaryngol. Head Neck Surg., *116:* 1394–1398, 1990.

35. Leonard, J. H., Kearsley, J. H., Chenevix-Trench, G., and Hayward, N. K. Analysis of gene amplification in head-and-neck squamous-cell carcinoma. Int. J. Cancer, *48:* 511–515, 1991.

36. Garte, S. J. The c-*myc* oncogene in tumor progression. Crit. Rev. Oncog., *4:* 435–449, 1993.

37. Fracchiolla, N. S., Pignataro, L., Capaccio, P., Trecca, D., Boletini, A., Ottaviani, A., Polli, E., Maiolo, A. T., and Neri, A. Multiple genetic lesions in laryngeal squamous cell carcinomas. Cancer (Phila.), *75:* 1292–1301, 1995.

38. Courjal, F., Cuny, M., Simonylafontaine, J., Louason, G., Speiser, P., Zeillinger, R., Rodriguez, C., and Theillet, C. Mapping of DNA amplifications at 15 chromosomal localizations in 1875 breast tumors—definition of phenotypic groups. Cancer Res., *57:* 4360–4367, 1997.

39. Field, J. K., Spandidos, D. A., Stell, P. M., Vaughan, E. D., Evan, G. I., and Moore, J. P. Elevated expression of the c-MYC oncoprotein correlates with poor prognosis in head and neck squamous cell carcinoma. Oncogene, *4:* 1463–1468, 1989.

40. Eversole, L. R., and Sapp, J. P. c-MYC oncoprotein expression in oral precancerous and early cancerous lesions. Eur. J. Cancer, *29B:* 131–135, 1993.

41. Porter, M. J., Field, J. K., Leung, S. F., Lo, D., Lee, J. C., Spandidos, D. A., and van Hasselt, C. A. The detection of the c-*myc* and *ras* oncogenes in nasopharyngeal carcinoma by immunohistochemistry. Acta Otolaryngol., *114:* 105–109, 1994.

42. Bos, J. L. RAS oncogenes in human cancer: a review. Cancer Res., *49:* 4682–4689, 1989.

43. Grandori, C., and Eisenman, R. N. *Myc* target genes. Trends Biochem. Sci., *22:* 177–181, 1997.

44. Shim, H., Lewis, B. C., Dolde, C., Li, Q., Wu, C. S., Chun, Y. S., and Dang, C. V. *Myc* target genes in neoplastic transformation. Curr. Top. Microbiol. Immunol., *224:* 181–190, 1997.

45. Fischer, R. S., and Quinlan, M. P. Identification of a novel mechanism of regulation of the adherens junction by E1A, RAC1, and cortical actin filaments that contributes to tumor progression. Cell Growth Differ., *9:* 905–918, 1998.

46. Goudie, D. R., Yuille, M. A., Leversha, M. A., Furlong, R. A., Carter, N. P., Lush, M. J., Affara, N. A., and Ferguson-Smith, M. A. Multiple self-healing squamous epitheliomata (ESS1) mapped to chromosome 9q22–q31 in families with common ancestry. Nat. Genet., *3:* 165–169, 1993.

47. Richards, F. M., Goudie, D. R., Cooper, W. N., Jene, Q., Barroso, I., Wicking, C., Wainwright, B. J., and Ferguson-Smith, M. A. Mapping the multiple self-healing squamous epithelioma (*MSSE*) gene and investigation of xeroderma pigmentosum group a (*XPA*) and patched (*PTCH*) as candidate genes. Hum. Genet., *101:* 317–322, 1997.

48. Shields, J. M., and Yang, V. W. Identification of the DNA sequence that interacts with the gut-enriched Krüppel-like factor. Nucleic Acids Res., *26:* 796–802, 1998.

49. Shields, J. M., and Yang, V. W. Two potent nuclear localization signals in the gut-enriched Krüppel-like factor define a subfamily of closely related Krüppel proteins. J. Biol. Chem., *272:* 18504–18507, 1997.

50. Jenkins, T. D., Opitz, O. G., Okano, J., and Rustgi, A. K. Transactivation of the human keratin 4 and Epstein-Barr virus ED-L2 promoters by gut-enriched Krüppel-like factor. J. Biol. Chem., *273:* 10747–10754, 1998.

51. Tonthat, H., Kaestner, K. H., Shields, J. M., Mahatanankoon, C. S., and Yang, V. W. Expression of the gut-enriched Krüppel-like factor gene during development and intestinal tumorigenesis. FEBS Lett., *419:* 239–243, 1997.

52. Miller, I. J., and Bieker, J. J. A novel, erythroid cell-specific murine transcription factor that binds to the CACCC element and is related to the Krüppel family of nuclear proteins. Mol. Cell. Biol., *13:* 2776–2786, 1993.

53. Kuo, C. T., Veselits, M. L., and Leiden, J. M. LKLF: a transcriptional regulator of single-positive T cell quiescence and survival. Science (Washington DC), *277:* 1986–1990, 1997.

54. Johnson, R. L., Rothman, A. L., Xie, J., Goodrich, L. V., Bare, J. W., Bonifas, J. M., Quinn, A. G., Myers, R. M., Cox, D. R., Epstein, E. H., Jr., and Scott, M. P. Human homolog of patched, a candidate gene for the basal cell nevus syndrome. Science (Washington DC), *272:* 1668–1671, 1996.

55. Fuchs, E., and Byrne, C. The epidermis: rising to the surface. Curr. Opin. Genet. Dev., *4:* 725–736, 1994.

56. Gandarillas, A., and Watt, F. M. c-Myc promotes differentiation of human epidermal stem cells. Genes Dev., *11:* 2869–2882, 1997.

57. Hueber, A. O., Zornig, M., Lyon, D., Suda, T., Nagata, S., and Evan, G. I. Requirement for the CD95 receptor-ligand pathway in c-MYC- induced apoptosis. Science (Washington DC), *278:* 1305–1309, 1997.

58. Brewster, R., Lee, J., and Ruiz i Altaba, A. Gli/zic factors pattern the neural plate by defining domains of cell differentiation. Nature (Lond.), *393:* 579–583, 1998.

59. Chomczynski, P., and Sacchi, N. Single-step method of RNA isolation by acid guanidinium thiocyanate-phenol-chloroform extraction. Anal. Biochem., *162:* 156–159, 1987.

60. Cheng, S., Schmidt-Grimminger, D. C., Murant, T., Broker, T. R., and Chow, L. T. Differentiation-dependent up-regulation of the human papillomavirus E7 gene reactivates cellular DNA replication in suprabasal differentiated keratinocytes. Genes Dev., *9:* 2335–2349, 1995.